OXFORD JOURNAL
OF STUDENT
SCHOLARSHIP

Quantitative Analysis of Basin-Boundary Complexity in Multi-Attractor Magnetic Pendulum Systems

Rishith Saraf
rishithsaraf290510@gmail.com

ABSTRACT

This study investigates the influence of magnet configuration on basin-boundary complexity in a simplified magnetic-pendulum-inspired system. The model considers a freely moving particle in a two-dimensional plane under the influence of multiple fixed magnetic attractors. Numerical simulations were performed by varying the number of attractors, N, from 2 to 5 and the radial distance, R, of the attractors from the centre of the system. For each configuration, basin-of-attraction maps were generated using a uniform grid of initial conditions, and a boundary-ratio metric was used to quantify the degree of basin complexity. The results show that increasing the number of attractors generally increases basin-boundary complexity and sensitivity to initial conditions. The N=2 system produced simple basin structures with a single dominant boundary, whereas systems with N=3, N=4, and N=5 exhibited increasingly interwoven and fragmented boundaries. However, maximum boundary complexity did not occur at the smallest radial spacing. Instead, the highest boundary ratios were observed at intermediate values of R, indicating that basin complexity is controlled by a balance between attractor separation and interaction strength. Nonlinear regression further indicated that the relationship between R and boundary complexity follows a systematic nonlinear trend. These findings suggest that attractor geometry plays a critical role in controlling predictability and basin-boundary formation in multi-attractor magnetic pendulum systems.

Keywords: Magnetic pendulum; Chaos theory; Basins of attraction; Boundary ratio; Nonlinear dynamics; Attractor configuration.

1. INTRODUCTION

Chaos theory provides a mathematical framework for understanding the behaviour of nonlinear dynamical systems. Dynamical systems describe how a system evolves with time under the influence of governing forces or equations. Classical dynamics has its foundation in Newtonian mechanics, which was originally developed to describe the motion of physical bodies, including celestial objects [1]. However, many nonlinear systems exhibit highly complex behaviour even when they are governed by deterministic equations. In such cases, small differences in the initial conditions can lead to significantly different outcomes over time. This sensitivity to initial conditions is one of the defining features of deterministic chaos [2].

Chaos and fractals are closely connected within the broader field of nonlinear dynamics. This field is concerned with systems that evolve with time and may reach a stable state, show periodic oscillations, or display complex and irregular behaviour [3]. Examples of dynamical systems are found in several areas, including classical mechanics, differential equations, chemical kinetics, fluid dynamics, biological systems, and population dynamics [4]. In many of these systems, the long-term behaviour is strongly influenced by attractors, which represent final states or regions towards which the system evolves.

Chaos theory has been widely used in physical, chemical, and biological sciences to study systems that are difficult to predict using simple linear models. Examples include turbulent flow in fluid dynamics, Brownian motion, molecular trajectories, population evolution, weather patterns, and biological rhythms [5]. Another well-known example of a deterministic chaotic system is the double pendulum. The double pendulum consists of two interconnected pendulums and is widely used as a classical example of nonlinear dynamics because small differences in the starting position can produce highly different motion paths [6]. Similarly, the magnetic pendulum provides a useful and visually clear system for studying deterministic chaos and basin-boundary formation [7].

A magnetic pendulum is a deterministic system in which the motion of a pendulum bob or moving particle is influenced by several fixed magnetic attractors. Although the governing equations are deterministic, the final outcome can be highly sensitive to the initial position of the particle. Two particles starting from nearly identical initial positions may eventually be captured by different magnets. This behaviour illustrates how unpredictability can arise in a system even when the underlying mathematical rules remain fixed [2,8].

In a magnetic pendulum system, each magnet competes to influence the final state of the moving particle. This competition produces regions known as basins of attraction. A basin of attraction is the set of initial conditions that eventually lead the particle to the same attractor [9]. When multiple attractors are present, the phase space is divided into different basins. The boundaries separating these basins may be smooth in simple systems, but in chaotic systems they can become highly irregular, fragmented, and interwoven. These complex boundaries are often associated with fractal basin structures, where neighbouring initial conditions may lead to different final attractors [10].

The structure of basin boundaries is important because it provides information about the predictability of the system. If the basin boundaries are smooth and well separated, the final attractor can be predicted with relatively high confidence. However, when the basin boundaries are highly complex, even a very small uncertainty in the initial condition can make the final outcome difficult to predict. Therefore, basin-boundary complexity provides a useful way to examine sensitivity to initial conditions in nonlinear dynamical systems [11].

Previous studies on magnetic pendulum systems have shown that chaotic motion, fractal basin boundaries, and sensitivity to initial conditions can arise depending on system parameters such as damping, forcing conditions, and attractor arrangement [12]. Basin structures are commonly assessed through visual inspection of colour-coded basin-of-attraction maps. While visual analysis is useful for identifying general trends, it is not sufficient on its own. Therefore, a numerical method is required to quantify basin-boundary complexity and compare the effects of different system parameters.

In this study, a numerical boundary-ratio metric was used to quantify the complexity of basin boundaries. The boundary ratio measures the extent to which neighbouring initial conditions evolve towards different attractors. A higher boundary ratio indicates greater basin complexity and increased sensitivity to initial conditions. This provides a quantitative measure of basin complexity and allows direct comparison between different magnet configurations.

Although earlier studies have examined chaotic behaviour in magnetic pendulum systems, comparatively less attention has been given to how the spatial arrangement of attractors influences the degree of basin-boundary complexity. In particular, the combined effects of the number of attractors and their radial distance from the centre have not been extensively quantified across multiple configurations. Since the interaction between neighbouring attractors governs the competition within the system, changing the spatial arrangement of magnets can significantly alter the predictability and complexity of the resulting basin structures.

Investigation on how magnet configuration influences basin-boundary complexity in a simplified magnetic-pendulum-inspired system was conducted. In contrast to a fully constrained physical pendulum, the model used considers a freely moving particle in a two-dimensional plane. This simplification was used to isolate the effect of attractor geometry on basin formation and boundary complexity. Numerical simulations were conducted by varying both the number of attractors and their radial distance from the centre of the system. Basin-of-attraction maps were generated for each configuration, and a boundary-ratio metric was used to quantify the degree of basin complexity. In addition, nonlinear regression analysis was performed to examine whether a systematic relationship exists between spatial configuration and boundary complexity.

The novelty of this work lies in quantitatively evaluating how the combined effects of attractor number and radial spacing influence basin-boundary complexity. By combining qualitative basin-map analysis with quantitative boundary-ratio measurements, it is possible to determine how attractor arrangement affects predictability and complex boundary formation in multi-attractor magnetic pendulum systems. The main objective is to determine whether an optimum spatial arrangement exists that maximises basin-boundary complexity.

It was hypothesised that basin-boundary complexity would increase as the number of attractors increases, due to the greater competition between possible final states. It was further hypothesised that the relationship between basin complexity and radial spacing would be non-monotonic, with maximum complexity occurring at intermediate magnet radii. At very small radii, the attractors were expected to behave as a closely clustered group, reducing effective competition, whereas at very large radii the attractors were expected to become too isolated to generate strongly interwoven basin boundaries. Therefore, the highest boundary complexity was expected to occur when the magnets were sufficiently separated to act as distinct attractors while still remaining close enough for strong dynamical competition between neighbouring basins.

2. METHODS

2.1. Model formulation and assumptions

The system was modelled as a simplified magnetic-pendulum-inspired dynamical system in which a point particle moves freely in a two-dimensional plane under the influence of multiple fixed magnetic attractors. Unlike a conventional magnetic pendulum, where the motion is constrained by a pendulum string and gravity, the present model considers an unconstrained particle moving in the $x - y$ plane. This simplification was adopted to isolate the nonlinear interaction between the moving particle and the fixed attractors, and to examine the resulting basin-of-attraction structures and sensitivity to initial conditions.

Several assumptions were introduced to reduce the model's complexity while preserving the system's essential nonlinear characteristics. First, the motion was restricted to two dimensions. Second, gravitational effects and pendulum-string constraints were neglected to avoid directional bias and to retain geometrical symmetry. Third, all magnetic attractors were assumed to have identical strength. Finally, the magnetic interaction was approximated using an inverse-cubic force law rather than a full electromagnetic field description. These assumptions allowed the system to be represented as a computationally manageable nonlinear dynamical model suitable for systematic parametric analysis.

The magnets were arranged symmetrically on a circle centred at the origin. For a system containing N magnets, the position of the i^{th} magnet was defined as:

$$M_i = \left(Rcos\frac{2\pi i}{N}, Rsin\frac{2\pi i}{N}\right), i = 0, 1, 2, ..., N - 1$$

where R is the radial distance of the magnets from the origin.

The motion of the particle was governed by the combined attractive force from all magnets and a damping term. The general form of the equation of motion can be written as:

$$m\frac{d^2r}{dt^2} = \sum_{i=1}^{N} \frac{k(M_i - r)}{\left(|M_i - r|^2 + \epsilon\right)^{3/2}} - c\frac{dr}{dt}$$

where r is the particle position, m is the particle mass, k is the magnetic attraction coefficient, c is the damping coefficient, and ϵ is a small regularisation parameter introduced to avoid numerical singularities when the particle approaches a magnet. Unit mass was assumed (m=1) for simplicity.

2.2. Numerical simulation and basin construction

The equations of motion were solved numerically using a time-stepping approach. At each time step, the particle's acceleration was calculated from the net force acting on it. The velocity and position were then updated using a first-order explicit Euler integration scheme:

$$v_{t+\Delta t} = v_t + a_t \Delta t r_{t+\Delta t} = r_t + v_{t+\Delta t}\Delta t$$

where v, a, and Δt represent the particle velocity, acceleration, and time step, respectively. A constant time step was used for all simulations to ensure consistency across the parameter space.

Each simulation was initiated from a prescribed starting position with an initial velocity of zero. The trajectory was advanced until either the particle was captured by one of the magnets or the maximum number of iterations was reached. A magnet was considered to have captured the particle when the distance between the particle and the magnet became smaller than a predefined capture radius. The corresponding magnet was then assigned as the final attractor for that initial condition.

To construct the basins of attraction, a uniform grid of initial conditions was defined over a square region of the two-dimensional plane. In the present study, a 500×500 grid was used, giving 250,000 independent initial points for each parameter combination. Each set of grid points was simulated independently for the different independent variables' values, and the final attractor was recorded in a two-dimensional array. The resulting basin maps were visualised by assigning a distinct colour to each attractor. Regions of uniform colour represent stable basins of attraction, whereas highly irregular or intermingled boundaries indicate strong sensitivity to initial conditions.

2.3. Experimental design

The parametric study focused on two primary independent variables: the number of magnets, N, and the radial distance of the magnets from the origin, R. The number of magnets was varied from 2 to 5 to examine the effect of increasing the number of competing attractors. Increasing N is expected to enhance the complexity of the system by increasing the number of possible final states and the degree of competition between attractors.

The radial distance R was varied from 0.25 to 1.50 units in increments of 0.25 units. Changing R modifies the spacing between the magnets, and therefore affects the balance between local attraction and competition among neighbouring attractors. All other model parameters, including the damping coefficient, magnetic force coefficient, integration time step, capture radius, and maximum number of iterations, were kept constant so that the individual effects of N and R could be isolated.

Table 1: Simulation parameters used in the computational model: The table lists the fixed numerical parameters and the ranges of the independent variables used to generate the basin maps and boundary-ratio data.

Parameter	Symbol	Value/range used	Comment
Magnet Number	N	2–5	Main independent variable
Magnet arrangement radius	R	0.25 – 1.50	Main independent variable, Step size = 0.25
Grid resolution	—	500×500	Initial-condition grid
Initial velocity	v_0	0	Same for all simulations
Time step	Δt	0.01	Euler Integration step
Damping coefficient	c	0.1	Controls energy loss
Magnetic coefficient	k	1	Force scaling constant
Capture radius	r_c	0.05	Defines attractor capture
Maximum iterations	—	10000	Stopping criterion
Domain size	—	$x, y\in[-\ 2,\ 2]$	simulation region

2.4. Boundary-ratio analysis

To quantify the complexity of the basin boundaries, a boundary ratio was calculated from each basin map. The boundary ratio measures the fraction of neighbouring grid-point pairs that belong to different attractors. A high boundary ratio indicates that adjacent initial conditions often evolve towards different final attractors, which is characteristic of strong sensitivity to initial conditions and more complex basin structures.

For a basin map represented by a two-dimensional array $B(i, j)$, the boundary ratio was calculated as:

$$Boundary\ ratio\ = \frac{\sum_{i=1}^{n_x-1}\sum_{j=1}^{n_y}[B(i,j)\neq B(i+1,j)]+\sum_{i=1}^{n_x}\sum_{j=1}^{n_y-1}[B(i,j)\neq B(i,j+1)]}{\left(n_x-1\right)\left(n_y\right)+\left(n_y-1\right)\left(n_x\right)}$$

where $B(i, j)$is the attractor assigned to the grid point (j), n_x and $n_y$are the number of grid points in the x and y directions, respectively, and [ ] is an indicator function that equals 1 when the condition is true and 0 otherwise. Each grid point was compared only with one horizontal and one vertical neighbouring point to avoid duplicate counting. Larger boundary-ratio values, therefore, correspond to more fragmented and interwoven basin boundaries.

2.5. Model validation and numerical checks

Several validation checks were performed to ensure that the numerical procedure and boundary-ratio calculation were consistent. First, simulations were conducted under limiting magnet-spacing conditions. When the magnets were positioned relatively far apart, the basin maps showed larger uniform regions and lower boundary-ratio values. In contrast, closer magnet spacing produced more complex basins and higher boundary-ratio values, consistent with the expected increase in attractor competition.

Second, the boundary-ratio algorithm was tested using predefined synthetic patterns, including uniform arrays and checkerboard-like configurations. Uniform arrays produced boundary-ratio values as zero, whereas alternating patterns produced boundary-ratio as 1, confirming that the algorithm correctly identified boundary-dominated structures.

Finally, the numerical boundary-ratio values were compared with the visual appearance of the corresponding basin maps. Basin maps with smooth and well-separated regions produced lower boundary ratios, while maps with irregular and highly complex boundaries produced higher values. These checks confirmed that the computational framework captured the qualitative and quantitative features of the nonlinear system.

The simplified model used in this study was not intended to reproduce the exact motion of a physical magnetic pendulum, but rather to isolate the effect of attractor configuration on basin formation and basin complexity. By modelling the system as a freely moving particle in a two-dimensional plane, the influence of the number of attractors and their radial arrangement could be examined without the additional complexity introduced by pendulum-length constraints, gravitational restoring forces, or three-dimensional motion. This reduction allowed the role of attractor geometry in shaping basin boundaries to be studied more directly. To ensure that the numerical results were not dominated by computational choices, sensitivity checks were carried out on the numerical setup. Basin maps and boundary-ratio values were compared under changes in grid resolution, and the qualitative trends remained unchanged. In particular, the observed increase in basin complexity with attractor number and the appearance of maximum complexity at intermediate magnet spacing were preserved across the tested numerical settings. This indicates that the main conclusions of the study are robust to reasonable variations in numerical resolution and integration parameters, and are therefore not artefacts of a single computational choice.

3. RESULTS AND DISCUSSION

3.1. Effect of magnet spacing on basin morphology

The basin-of-attraction maps showed a clear dependence on the radial distance, R, between the magnets and the centre of the system. At smaller radial distances, the attractors were positioned close to one another, resulting in strong overlap between their regions of influence. Under these conditions, the particle experienced a combined attractive field rather than well-separated competing forces. Consequently, the basin structures appeared less fragmented, particularly when the magnets were closely clustered near the origin, as observed in Figure 1(A).

As R increased, the attractors became more spatially separated, which modified the competition between neighbouring magnets. At intermediate values of R, the basin boundaries became more irregular and interwoven, indicating increased sensitivity to the initial conditions. This behaviour suggests that complex boundary formation is promoted when the attractors are sufficiently separated to act as distinct final states, while still remaining close enough to interact strongly with one another, as visible in Figures 1(B) and 1(C).

At larger values of R, the basin boundaries became smoother and more clearly separated. This reduction in boundary irregularity indicates that the interaction between magnets weakened as the spacing increased. As a result, each attractor dominated a more localised region of the domain, reducing the degree of basin complexity, as shown in Figures 1(D), 1(E) and 1(F).

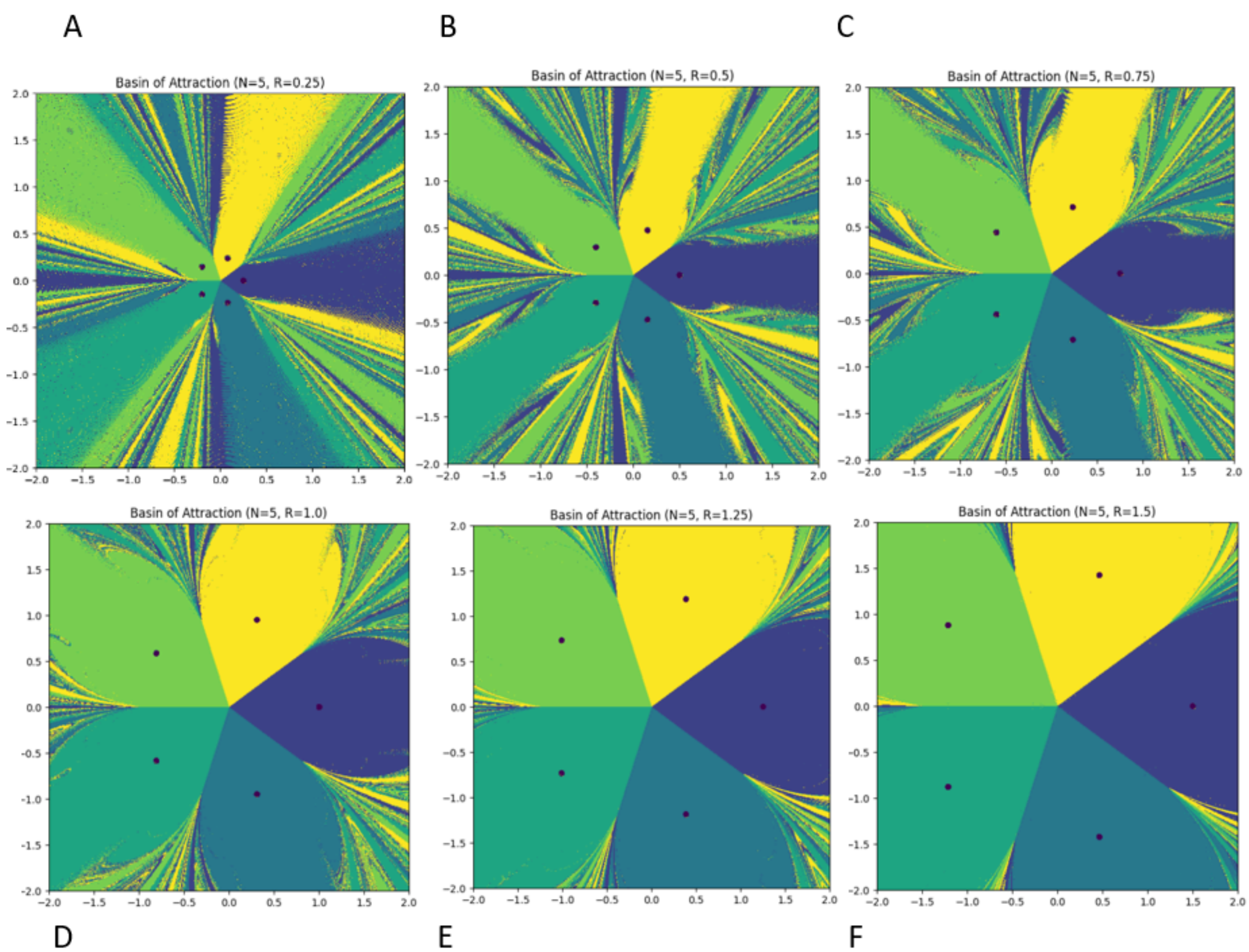

Figure 1. Basin-of-attraction maps for the five-magnet system (N=5), at six magnet arrangement radii: (A) R=0.25, (B) R=0.5, (C) R=0.75, (D) R=1.0, (E) R=1.25, (F) R=1.5. Each coloured point represents

the final attractor reached by a particle released from a given initial condition in the (x, y) plane, where the horizontal and vertical axes denote the initial x and y coordinates, respectively.

3.2. Effect of the number of attractors on basin complexity

Increasing the number of magnets from $N = 2$ to $N = 5$ produced a noticeable increase in the complexity of the basin-of-attraction structures. For $N = 2$, the basin maps were relatively simple across all radial distances. Only one dominant boundary separating the two attractor regions was observed, and complex fragmentation was largely absent, as shown in Figure 2(A). This was also reflected in the very low boundary-ratio values obtained for $N = 2$ as shown in Table 2.

For $N = 3$, the introduction of an additional attractor increased the competition within the system, producing more irregular boundary regions compared with the two-magnet case. The basin maps showed greater sensitivity to initial conditions, with more frequent changes in the final attractor across neighbouring grid points, as visible in Figure 2(B).

Further increases in the number of magnets to $N = 4$ and $N = 5$ resulted in more complex basin structures. The additional attractors increased the number of competing final states, which promoted more complex boundary formation, as observed in Figures 2(C) and 2(D). However, the increase in complexity was not linear with N. At $R = 0.5$, the boundary ratio increased from 0.003727 for $N = 2$ to 0.107531 for $N = 3$, 0.237988 for $N = 4$, and 0.251842 for $N = 5$. The change in boundary complexity from N = 2 to N = 3 was more pronounced than the change from N = 3 to N = 4, indicating that the rate of increase in complexity decreases as more attractors are added.

This suggests that the number of attractors is an important control parameter for boundary formation. However, beyond a certain number of attractors, the addition of further magnets does not increase the complexity at the same rate, most likely because the available spatial domain is already strongly divided among competing basins.

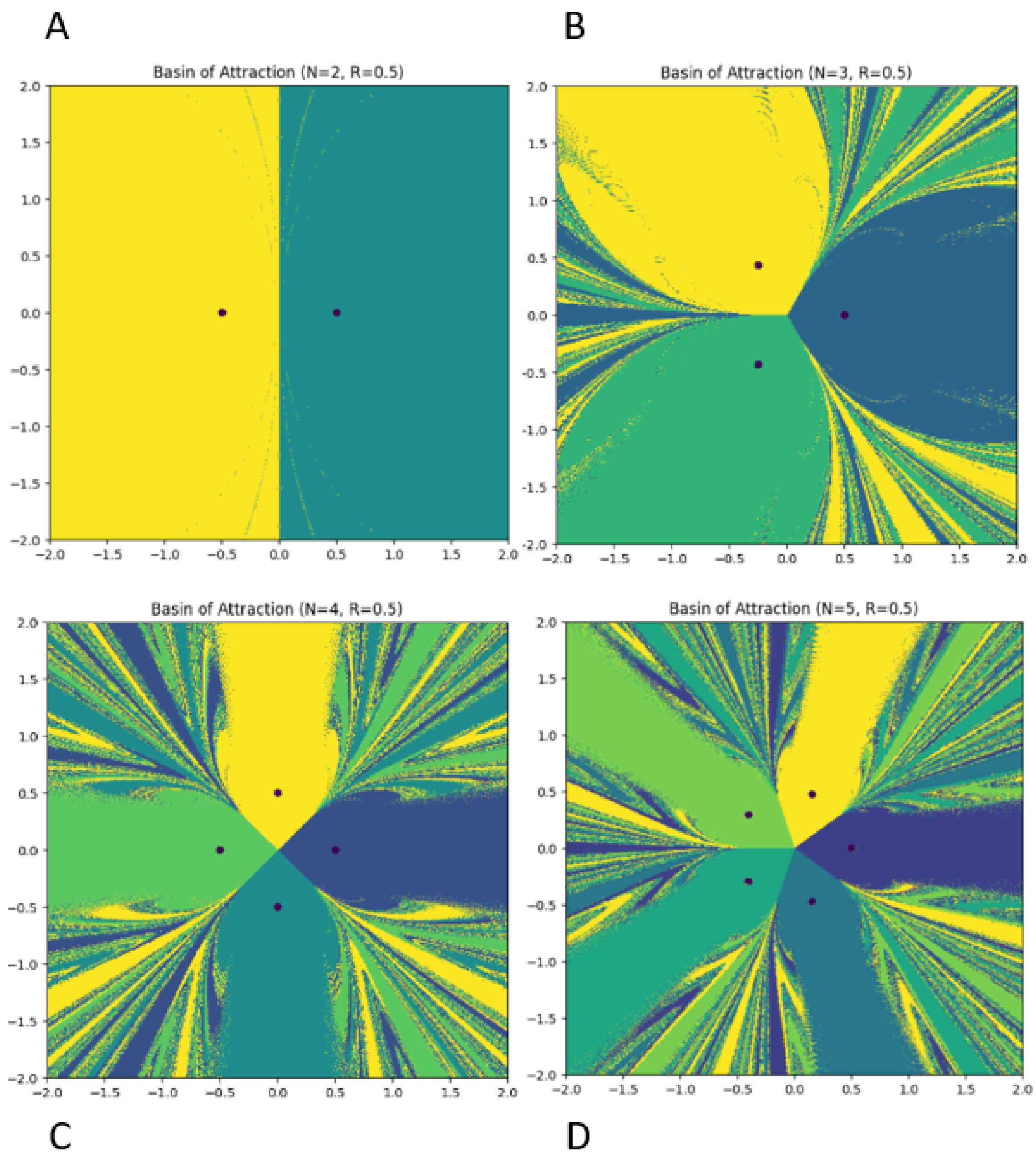

Figure 2. Basin-of-attraction maps for magnetic pendulum systems with (A) N = 2, (B) N = 3, (C) N = 4, and (D) N = 5 magnets, all evaluated at a common magnet radius of R = 0.50. Each colour denotes a different final attractor basin, and the coloured dots mark the magnet locations. The horizontal and vertical axes represent the initial particle coordinates x_0 and y_0, respectively, over the simulation domain [-2,2] × [-2,2]. The figure illustrates the progressive increase in basin-boundary complexity as the number of competing attractors increases, with the two-magnet case showing a simple dividing boundary and the higher-N cases displaying increasingly fragmented and interwoven basin structures.

3.3. Boundary-ratio variation with radial distance

The quantitative boundary-ratio analysis supported the trends observed in the basin maps. For $N = 2$, the boundary-ratio values remained very low across all radial distances, confirming the limited fragmentation of the basin boundary. This is expected because only two final attractors compete in the system, producing a relatively simple division of the initial-condition space.

For higher numbers of magnets, the boundary ratio increased, indicating greater intermixing between basins. However, the maximum boundary ratio was not always observed at the smallest radial distance. In particular, for $N = 4$ and $N = 5$, the highest boundary complexity occurred at intermediate values of R, as visible in Figures 1(B) and 3(B). This non-monotonic trend indicates that boundary complexity is controlled by a balance between attractor proximity and attractor separation.

At very small values of R, the magnets were positioned close together and effectively behaved as a strongly clustered group, as shown in Figure 3(A). In this configuration, the system behaves more like a reduced-attractor system, resulting in lower boundary complexity. At intermediate R, the magnets were sufficiently separated to act as distinct attractors, while still interacting strongly enough to generate competition between basins. This produced the highest degree of boundary complexity, as observed in Figure 3(B). At large R, the magnets become more isolated, weakening the interaction between attractors and producing smoother and less complex basin boundaries, as visible in Figures 3(C), 3(D), 3(E) and 3(F). Therefore, the boundary-ratio results reveal the existence of an optimum spatial configuration for maximising basin-boundary complexity.

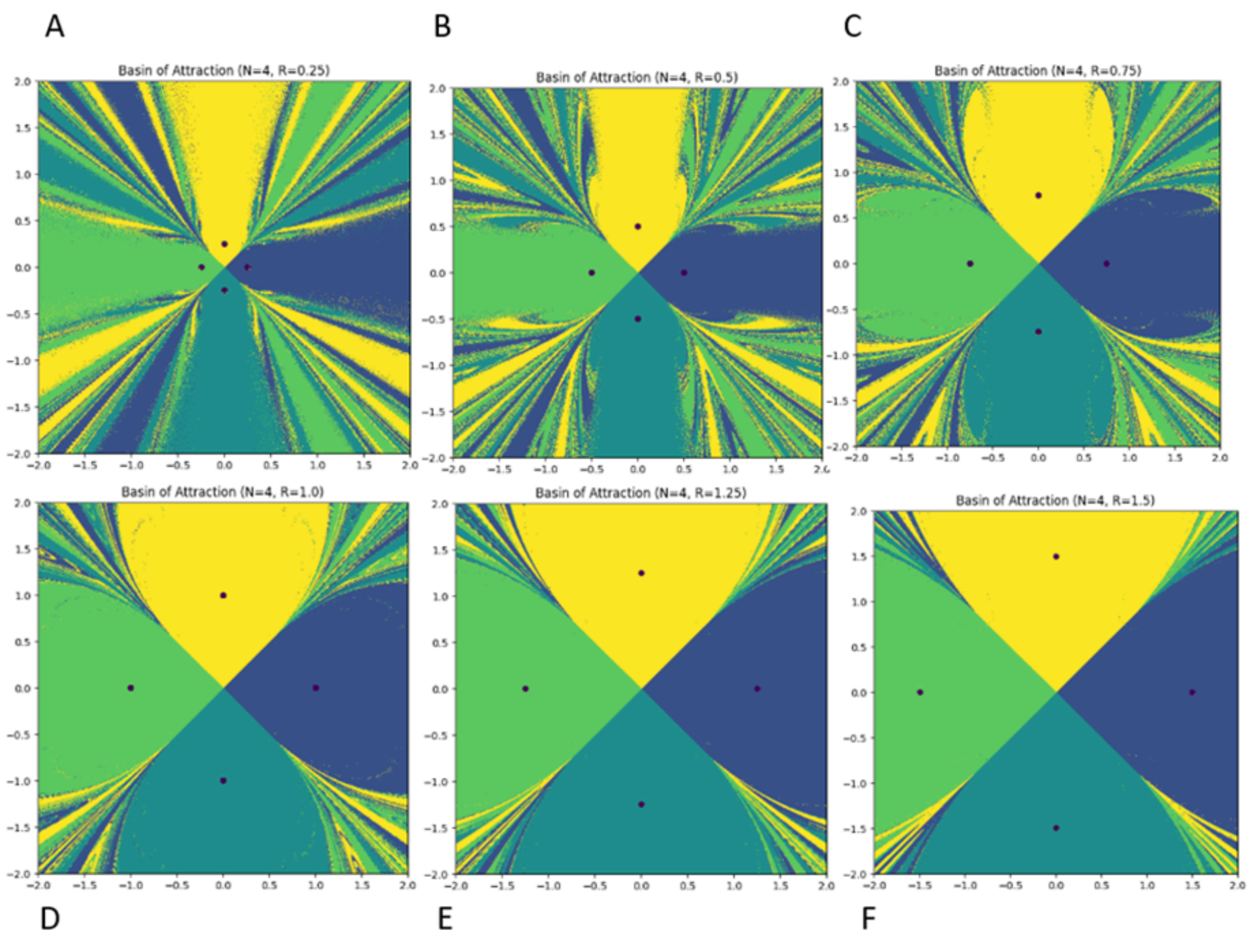

Figure 3. Basin-of-attraction maps for the four-magnet system (N=4), at six magnet arrangement radii: (A) R=0.25, (B) R=0.5, (C) R=0.75, (D) R=1.0, (E) R=1.25, (F) R=1.5. Each coloured point represents the final attractor reached by a particle released from a given initial condition in the (x, y) plane, where the horizontal and vertical axes denote the initial x and y coordinates, respectively.

3.4. Identification of an optimum radius for complex boundary formation

One of the most important findings of this study is that maximum basin complexity occurs at intermediate radial distances rather than at the smallest radial distances. This behaviour can be interpreted in terms of three regimes:

Small R**:** clustered attractors and reduced effective competition.

Intermediate R**:** strong interaction between attractors, sufficient spatial separation, and maximum basin-boundary complexity.

Large R**:** isolated attractors and smoother basin boundaries.

The existence of an intermediate-radius maximum suggests that the spatial arrangement of attractors can be tuned to control the complexity of the system. This result is important because it shows that boundary formation is governed not only by the number of attractors, but also by their geometrical arrangement.

The optimum boundary ratio also shifts with the number of magnets. For $N = 4$ and $N = 5$, the highest boundary ratio among the tested radii occurred at $R = 0.5$, with values of 0.237988 and 0.251842, respectively. However, because R was sampled at discrete intervals, these values should be interpreted as the optimum radii within the tested range, rather than exact global optima.

3.5. Additional investigation for the three-magnet system

The observation of maximum complexity at intermediate values of R for $N = 4$ and $N = 5$ motivated a closer examination of the three-magnet system. Since $N = 3$ contains fewer competing attractors, the radius corresponding to maximum boundary complexity was expected to occur at a smaller value of R than that observed for the four and five-magnet systems.

To test this possibility, additional simulations were performed at smaller radial distances for $N = 3$. If a similar non-monotonic trend is observed, it would indicate that the optimum radius for maximum boundary complexity shifts depending on the number of attractors. This would further support the conclusion that complex basin formation is controlled by the balance between attractor separation and interaction strength.

After inspecting Figures 4(A) and 4(B), and considering the trends observed for $N = 4$ and $N = 5$, it was suspected that the optimum boundary ratio for $N = 3$ lies between $R = 0.25$ and $R = 0.5$.

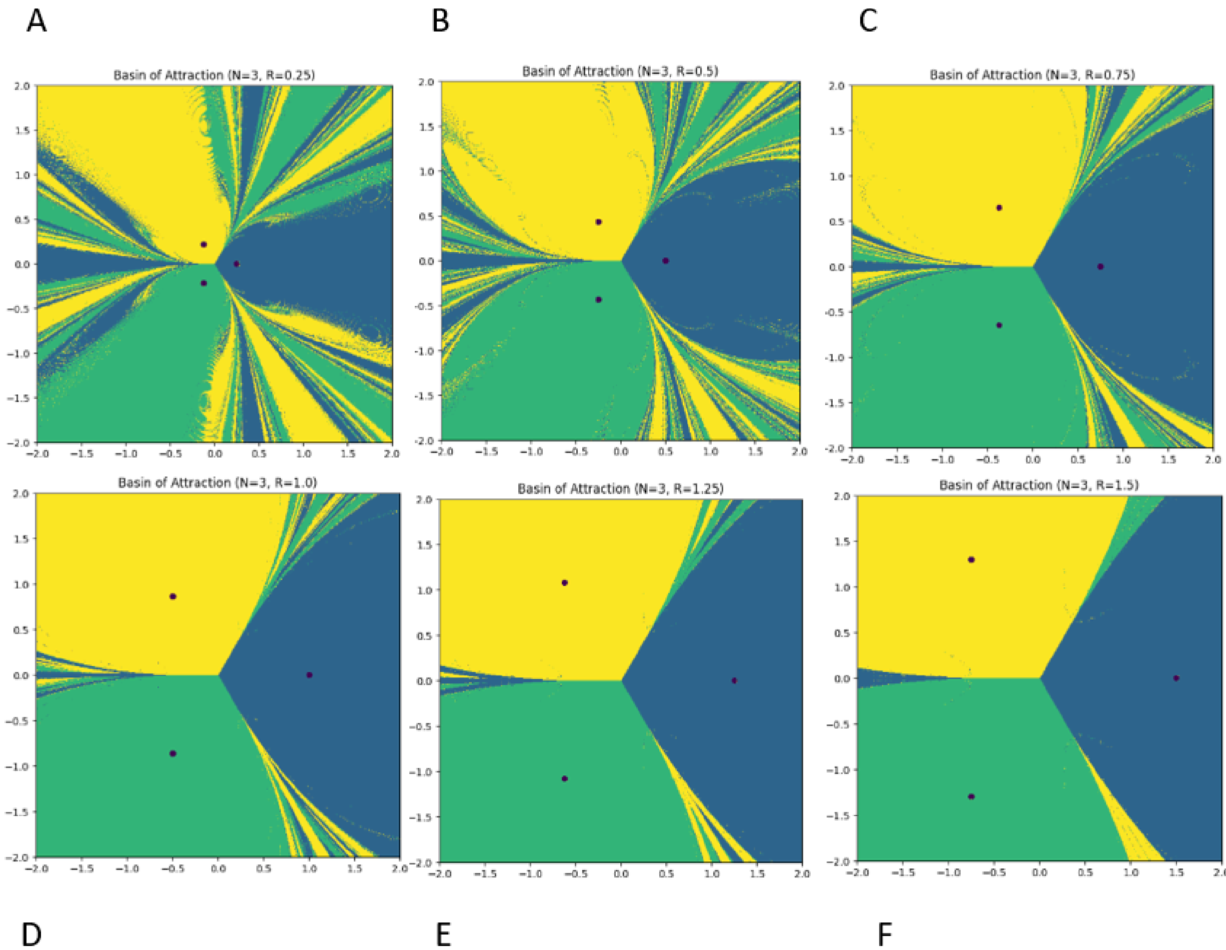

Figure 4. Basin-of-attraction maps for the three-magnet system (N=3), at six magnet arrangement radii: (A) R=0.25, (B) R=0.5, (C) R=0.75, (D) R=1.0, (E) R=1.25, (F) R=1.5. Each coloured point represents the final attractor reached by a particle released from a given initial condition in the (x, y) plane, where the horizontal and vertical axes denote the initial x and y coordinates, respectively.

3.6. Additional simulations for $N = 3$

Additional simulations were carried out for the three-magnet system at intermediate radii (R = 0.35, 0.375, and 0.40) to examine the region near the observed maximum in basin complexity more closely. These supplementary basin maps showed that the increase in boundary complexity was not abrupt, but occurred over a narrow range of intermediate radii where the attractors were sufficiently separated to behave as distinct final states while still remaining close enough to interact strongly. The results therefore support the broader conclusion that basin complexity is maximised at intermediate magnet spacing, rather than at the smallest or largest radii considered.

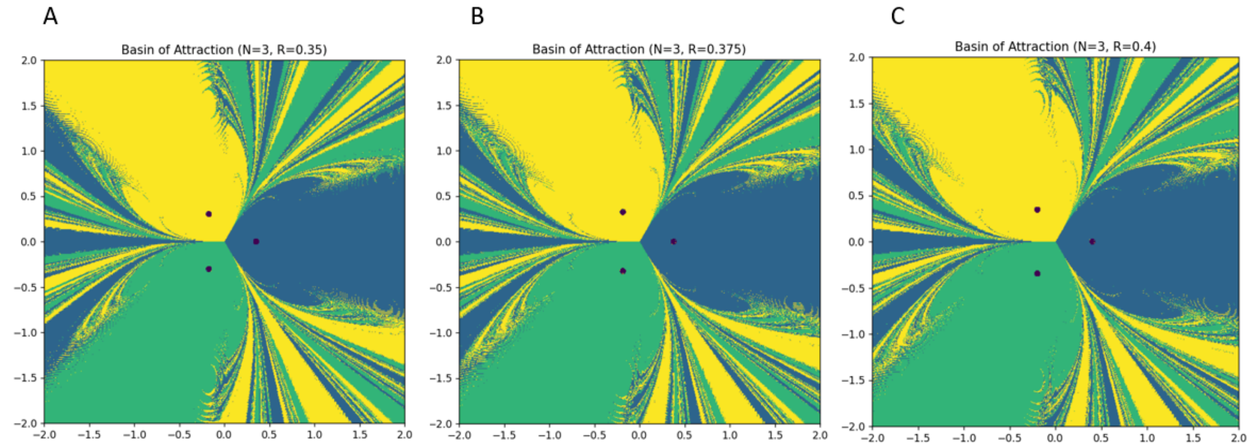

Figure 5. Basin-of-attraction maps for a magnetic pendulum system with N = 3 magnets, shown for (A) R = 0.35, (B) R = 0.375, and (C) R = 0.40. Each coloured region represents the set of initial conditions that converge to one of the three attractors, while the small dots indicate the magnet positions. The horizontal and vertical axes correspond to the initial particle coordinates x and y, respectively, over the domain [-2,2] × [-2,2]. These additional simulations were performed near the region of peak boundary complexity in order to examine the variation of basin complexity more closely as the magnet radius changes through intermediate values.

3.7. Exclusion of additional simulations for $N = 2$

Additional simulations were not performed for the $N = 2$ system because the basin structures remained comparatively simple across all investigated radii, as observed in Figure 6. The boundary-ratio values were consistently very small, indicating minimal fragmentation and weak sensitivity to initial conditions. Furthermore, even at low values of R, the basin maps exhibited a single clear dividing boundary between the two attractors rather than the complex interwoven structures observed for higher values of N. As a result, further refinement of the parameter range for $N = 2$ was unlikely to provide significant additional insight into complex basin-boundary formation.

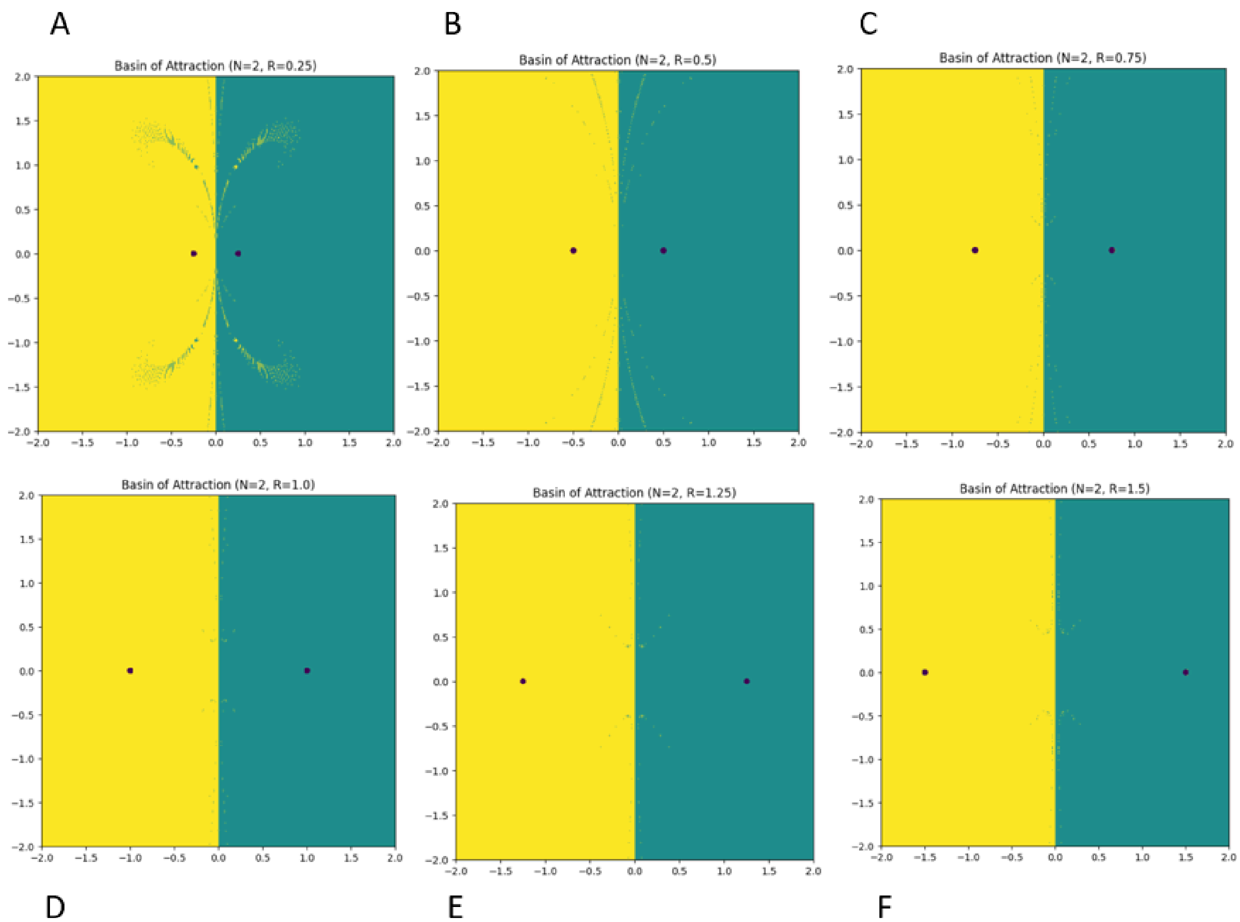

Figure 6. Basin-of-attraction maps for the two-magnet system (N=2), at six magnet arrangement radii: (A) R=0.25, (B) R=0.5, (C) R=0.75, (D) R=1.0, (E) R=1.25, (F) R=1.5. Each coloured point represents the final attractor reached by a particle released from a given initial condition in the (x, y) plane, where the horizontal and vertical axes denote the initial x and y coordinates, respectively.

3.8. Nonlinear regression analysis

To further investigate the relationship between boundary complexity and arrangement radius, nonlinear regression analysis was performed on the boundary-ratio data for systems with $N = 3$, $N = 4$, and $N = 5$. In all three cases, the data could be accurately approximated using a nonlinear model of the form:

$$B(R) \sim AR^{a}e^{-bR}$$

where $B(R)$ represents the boundary ratio, R is the arrangement radius, and A, a, and b are empirical fitting constants obtained through regression analysis.

The fitted curves showed strong agreement with the simulation data across all investigated systems. Example regression fits for the $N = 3$, $N = 4$, and $N = 5$ configurations are shown in Figures 7(A), 7(B), and 7(C), respectively. The corresponding coefficients of determination were $R^2 = 0.9916$, $R^2 = 0.9997$, and $R^2 = 0.9807$, indicating that the proposed nonlinear model closely reproduces the observed behaviour of the system.

The nonlinear regression model captures the competing mechanisms influencing basin-boundary complexity. The power-law term R^a describes the initial increase in complexity as neighbouring attractors become sufficiently separated to form distinct competing regions. In contrast, the exponential decay term e^{-bR} represents the gradual weakening of inter-attractor interaction at larger spatial separations. Together, these effects naturally produce a maximum boundary complexity at intermediate values of R, consistent with the trends observed in the basin maps and boundary-ratio measurements.

Although the regression model was derived empirically and is not proposed as a universal law for all chaotic attractor systems, the consistent agreement across multiple values of N suggests that the relationship between spatial configuration and basin-boundary complexity follows a systematic nonlinear trend within the parameter range investigated in this study.

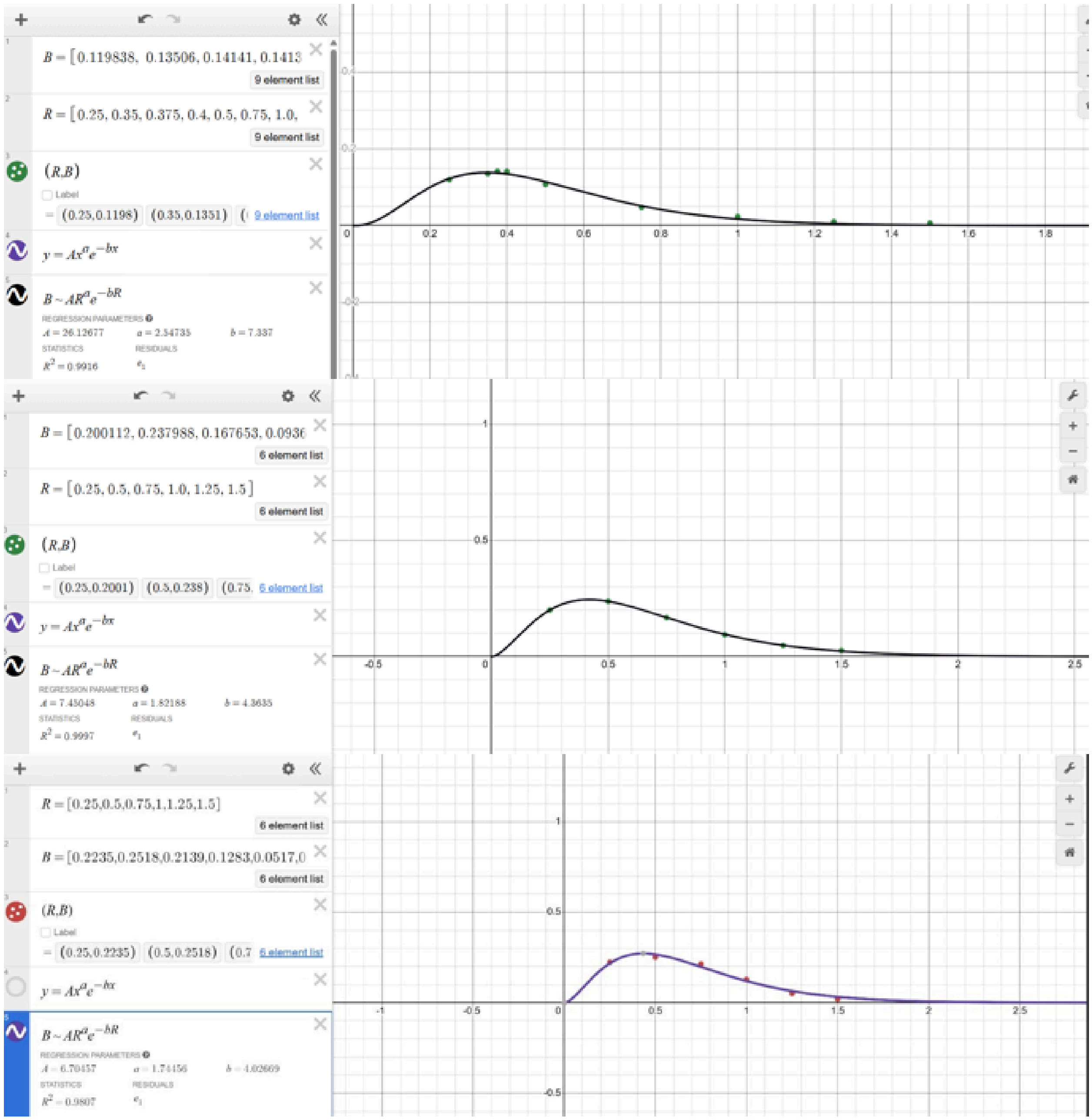

Figure 7. Nonlinear regression curves for the boundary-ratio data of magnetic pendulum systems with (A) N = 3, (B) N = 4, and (C) N = 5 magnets. In each panel, the data points show the numerically computed boundary-ratio values for different magnet radii R, and the solid curve shows the fitted model of the form $B(R) \sim AR^{a}e^{-bR}$, where B is the boundary ratio and A, a, and b are fitted constants. The horizontal axis represents the magnet arrangement radius R, and the vertical axis represents the computed boundary ratio. The fitted curves capture the non-monotonic dependence of basin-boundary complexity on magnet spacing, with boundary complexity increasing to a maximum at intermediate radii and then decreasing as the magnets become more widely separated.

3.9. Limitations, physical interpretation, and generalisation

The observation that maximum basin complexity is found at intermediate magnet spacing can be understood as a consequence of the balance between attractor overlap and attractor separation. When the magnet radius is very small, the attractors are tightly clustered and their regions of influence overlap strongly. In this situation, the system behaves less like a set of well-separated competing attractors and more like a strongly grouped attractor configuration, reducing the number of effectively distinct competing final magnets. As a result, the basin boundaries are less fragmented and the overall basin complexity remains relatively low. At intermediate magnet radii, however, the attractors become sufficiently separated to act as distinct final states while still remaining close enough for their regions of influence to overlap substantially. This creates a regime of strong competition in which small changes in the initial condition can alter which attractor ultimately captures the particle, leading to highly interwoven basin boundaries and a peak in basin complexity. When the radius becomes large, the magnets are spaced too far apart for strong overlap to persist, so each attractor dominates a more localised region of the plane and the basin boundaries become smoother. Therefore, the non-monotonic relationship between radius and basin complexity reflects a competition between clustering and isolation, with maximum complexity emerging when the attractors are distinct but still strongly interacting.

Although the system captures the essential competition between multiple attractors, several simplifying assumptions limit the direct quantitative applicability of the findings to real magnetic pendulum systems. First, the motion was represented as that of a freely moving particle in a two-dimensional plane rather than a pendulum bob constrained by a string. This removes the geometric restriction imposed by pendulum motion and allows trajectories that would not occur in a real suspended pendulum. Second, gravitational restoring forces were omitted. In a physical magnetic pendulum, gravity contributes to the restoring motion of the bob and introduces an additional force balance that may alter basin shapes and shift the radial position at which maximum basin complexity occurs. Third, all magnets were assumed to have identical strength and were placed in perfectly symmetric configurations. In real systems, slight asymmetries in magnet strength, placement, or alignment could distort basin boundaries, bias the size of particular basins, and modify the degree of competition between attractors. These assumptions mean that the numerical boundary-ratio values and the precise radius at which maximum complexity occurs should not be interpreted as universal quantitative predictions for experimental systems. Instead, the results are best understood as describing an idealised multi-attractor system in which the influence of attractor geometry can be isolated. Nevertheless, the broader qualitative conclusion is expected to remain relevant beyond this specific setup: basin complexity in chaotic multi-attractor systems is strongly governed by the balance between attractor proximity and attractor separation. Systems in which attractors are too closely clustered may behave as though fewer effective attractors are present, while systems in which attractors are too widely separated may exhibit weaker competition and smoother basin boundaries. In this sense, the study provides a simplified framework for understanding how spatial arrangement can influence predictability and basin formation in chaotic systems, even though the exact numerical results remain model-dependent.

Table 2: Boundary ratio table: Boundary-ratio values computed for magnetic pendulum systems with different numbers of magnets (N) and magnet arrangement radii (R).

Number magnets, N	**Radius,** R	**Boundary ratio**	**Main observation**
2	0.25	0.009587	One clear boundary with little fragmentation
2	0.50	0.003727	One clear boundary with little fragmentation
2	0.75	0.002228	One clear boundary with negligible fragmentation
2	1.00	0.001876	One clear boundary with negligible fragmentation
2	1.25	0.001852	One clear boundary with negligible fragmentation
2	1.50	0.002012	One clear boundary with negligible fragmentation
3	0.25	0.119838	Moderate basin complexity
3	0.35	0.135060	Additional investigation; high boundary complexity
3	0.375	0.141410	Additional investigation; highest boundary complexity for $N = 3$
3	0.40	0.141340	Additional investigation; close to the highest boundary complexity
3	0.50	0.107531	Strong attractor competition
3	0.75	0.047451	Reduced fragmentation
3	1.00	0.023202	More separated basins
3	1.25	0.010170	Low boundary complexity
3	1.50	0.006375	Weak intermixing
4	0.25	0.200112	Highly fragmented boundaries
4	0.50	0.237988	Highest overall complexity for $N = 4$ within the tested radii
4	0.75	0.167653	High basin complexity
4	1.00	0.093667	Moderate fragmentation
4	1.25	0.047046	Reduced boundary complexity

Number magnets, N	Radius, R	Boundary ratio	Main observation
4	1.50	0.025164	Mostly separated attractors
5	0.25	0.223515	Strong fragmentation
5	0.50	0.251842	Highest overall complexity for $N = 5$ within the tested radii
5	0.75	0.213940	Significant basin complexity
5	1.00	0.128295	Moderate-to-high complexity
5	1.25	0.051727	Reduced interweaving
5	1.50	0.020072	Low fragmentation due to increased separation

4. CONCLUSION

This study examined the influence of magnet configuration on basin-boundary complexity in a simplified magnetic-pendulum system. Numerical simulations were performed by varying the number of attractors and their radial distance from the centre, while basin-of-attraction maps and a boundary-ratio metric were used to quantify basin complexity.

The results show that both the number of attractors and their spatial arrangement strongly affect basin-boundary complexity. Increasing the number of magnets generally increased fragmentation and sensitivity to initial conditions, although the rate of increase reduced at higher values of N. The $N = 2$ system showed simple basin structures with a single dominant boundary, whereas systems with $N = 3$, $N = 4$, and $N = 5$ produced more interwoven and irregular boundaries.

A key finding is that maximum boundary complexity did not occur at the smallest magnet spacing, but at intermediate values of R. This indicates that basin complexity is controlled by a balance between attractor separation and interaction strength. At a very small radius, the magnets behave as a clustered group, while at a large radius, they become more isolated. Intermediate spacing provides the strongest competition between attractors and therefore produces the highest boundary complexity.

Nonlinear regression analysis further showed that the relationship between arrangement radius and boundary ratio follows a systematic nonlinear trend for $N = 3$, $N = 4$, and $N = 5$. This suggests that, although the system is sensitive to initial conditions, its basin-boundary complexity can still be quantified and described using reproducible mathematical trends.

The present model was intentionally simplified by considering two-dimensional motion, identical magnet strength, and no gravitational or pendulum-string constraints. Future work may extend this study by considering asymmetric magnet arrangements, unequal magnet strengths, three-dimensional motion, and additional chaos indicators such as Lyapunov exponents or fractal dimension analysis.

Supplementary Section
https://docs.google.com/document/d/1VTGpuXh4qGa8zhsv4KB7SE4Y-fLy7Q2z/edit?usp=sharing&ouid=113152063465588059913&rtpof=true&sd=true

REFERENCES

[1] C. Oestreicher, A history of chaos theory, Dialogues Clin. Neurosci. 9 (2007) 279–289. https://doi.org/10.31887/DCNS.2007.9.3/coestreicher.

[2] B. Qin, Y. Zhang, Comprehensive analysis of the mechanism of sensitivity to initial conditions and fractal basins of attraction in a novel variable-distance magnetic pendulum, Chaos Solitons Fractals 183 (2024) 114933. https://doi.org/10.1016/j.chaos.2024.114933.

[3] Thompson, John Michael Tutill, and H. Bruce Stewart. *Nonlinear dynamics and chaos*. John Wiley & Sons, 2002.

[4] J.E. Skinner, M. Molnar, T. Vybiral, M. Mitra, Application of chaos theory to biology and medicine, Integrative Physiological and Behavioral Science 27 (1992) 39–53. https://doi.org/10.1007/BF02691091.

[5] B. Qin, Y. Zhang, A novel global perspective: Characterizing the fractal basins of attraction and the level of chaos in a double pendulum, Chaos Solitons Fractals 189 (2024) 115694. https://doi.org/10.1016/j.chaos.2024.115694.

[6] C.H.. Skiadas, Charilaos. Skiadas, Handbook of Applications of Chaos Theory, 2017.

[7] S. Boccaletti, The control of chaos: theory and applications, Phys. Rep. 329 (2000) 103–197. https://doi.org/10.1016/S0370-1573(99)00096-4.

[8] H.E. Nusse, J.A. Yorke, E.J. Kostelich, Basins of Attraction, in: 1994: pp. 269–314. https://doi.org/10.1007/978-1-4684-0231-5_7.

[9] A. Wagemakers, Basins of Attraction: A Dynamical Zoo, (2025). https://doi.org/10.1142/S0218127425300241.

[10] G. Datseris, A. Wagemakers, Effortless estimation of basins of attraction, Chaos: An Interdisciplinary Journal of Nonlinear Science 32 (2022). https://doi.org/10.1063/5.0076568.

[11] S.W. McDonald, C. Grebogi, E. Ott, J.A. Yorke, Fractal basin boundaries, Physica D 17 (1985) 125–153. https://doi.org/10.1016/0167-2789(85)90001-6.

[12] J. Tobochnik, H. Gould, Quantifying Chaos, Computers in Physics 3 (1989) 86–90. https://doi.org/10.1063/1.4822881.